Paper:

Influencing Factors on Rotate Vector Reducer Dynamic Transmission Error

Shou-Song Jin, Xiao-Tao Tong, and Ya-Liang Wang[†]

College of Mechanical Engineering, Zhejiang University of Technology
No.288 Liuhe Road, Xihu District, Hangzhou, Zhejiang 310023, China
[†]Corresponding author, E-mail: wangyaliang@zjut.edu.cn
[Received December 15, 2018; accepted May 24, 2019]

The factors influencing rotate vector (RV) reducer dynamic transmission error were studied using virtual prototyping technology, which contained the elastic deformation, working load, part manufacturing error, and assembly clearance. According to the error transmission relationship of the RV reducer, 15 influencing factors were selected to design an orthogonal simulation test. The virtual prototype of the RV reducer was built using CREO and ANSYS, and imported into ADAMS for multi-body dynamics simulation. The simulation method reliability was verified via experiments. The results show that the circle center radius error of the pin gear, the amount of equidistant modification of the cycloid gear, the amount of radial-moving modification of the cycloid gear, the clearance between the support bushing and planet carrier, and the clearance between the crankshaft and the support bushing were positively correlated with the RV reducer dynamic transmission error. Among these, the circle center radius error of the pin gear has the greatest influence on the dynamic transmission error of the RV reducer followed by the amount of equidistant modification of the cycloid gear. The elastic deformation of the part and the load fluctuation show a certain gain effect on the transmission error, the elastic deformation of the cycloid gear has a great influence, and the elastic deformation of the pin gear has the least.

Keywords: RV reducer, dynamic transmission error, virtual prototyping, ANSYS, ADAMS

1. Introduction

The rotate vector (RV) reducer is a closed differential gear train composed of a planetary gear reducer and a cycloidal pin gear reducer. It is widely used in industrial robots, radars, precision machine tools, and other fields. As the core component of industrial robots, RV reducers account for approximately 34% of the total cost of robots. As the demand for industrial robots continues to increase, research regarding RV reducers is receiving increasing attention. Transmission error is an important indicator to measure RV reducer transmission performance. Scholars have conducted in-depth research and obtained excellent research results. Blanche and Yang studied the transmission of a cycloidal pinion planetary reducer using a pure geometric method [1, 2]. Hidaka used the mass spring equivalent model to study the influence of part machining error and assembly error on RV reducer static transmission error [3, 4]. Han comprehensively considered the machining error, installation error, clearance, and other factors of various parts of a system to establish a nonlinear dynamics calculation model of RV reducer dynamic transmission error and studied the model solving method [5]. He and Meng established the RV reducer dynamic model and the dynamic equilibrium equation by considering each single error, respectively. The maximum transmission error of an RV-40E reducer was obtained through experiments [6, 7]. Shan, Sun, Zhao, and Han established a mathematical model of transmission error based on part error and analyzed the sensitivity of the influential factors as well as studied the influence of each part error on the transmission error [8–11]. Li analyzed the relationship between machining tolerance and transmission error through programming calculation [12]. Chu proposed a matching algorithm based on a genetic algorithm for the assembly of an RV reducer which reduces the assembly clearance of parts and ensures RV reducer transmission precision [13]. Li combines the robust design and orthogonal test method to study the influence of the error of the RV reducer carrier on the transmission error [14].

With the development of computer simulation technology, some scholars have applied virtual prototype technology to research of the RV reducer transmission error. Wu comprehensively considered the clearance, machining error, assembly error, elastic deformation, and other factors to establish a virtual prototype model and verified the reliability of the virtual prototype through actual measurements [15]. Liu established a three-dimensional model of an RV reducer in a Unigraphics (UG) environment and imported ADAMS software for multi-body dynamics simulation [16]. The results show that the errors of cycloid gear modification, radius error, and radius error of the center circle of the pin have a great influence on transmission error. Zhu combined PRO/E, ANSYS, and ADAMS to establish a rigid-flexible coupled virtual prototype and analyzed the influence of clearance and elastic

deformation on RV reducer transmission error [17]. Li combined the orthogonal test method and virtual prototype technology to study the influence of five types of parts error on the transmission error of RV reducer and derived a transmission error calculation formula for the influencing factors [18].

The aforementioned literature organically combines virtual prototype technology with RV reducer transmission error and has achieved certain results; however, all of the studies are based on the study of static transmission error. The dynamic influence of the load on the RV reducer transmission error is not considered. The simulation environment and the actual working condition of the RV reducer are quite different, and the selection of other factors is not sufficiently comprehensive. In this study, the RV-40E type reducer is selected as the research object and the RV reducer angle error is used as the transmission error evaluation index. The virtual prototype model is established by combining CREO and ANSYS. The model was imported into ADAMS software for rigid-flexible coupling dynamics simulation. The effects of elastic deformation, working load size and fluctuation, part manufacturing error, and matching clearance on the dynamic transmission error of the RV reducer were studied. Wave load was added during the simulation. The simulation environment is nearer the actual RV reducer working condition, which provides a theoretical basis for further improving RV reducer transmission accuracy.

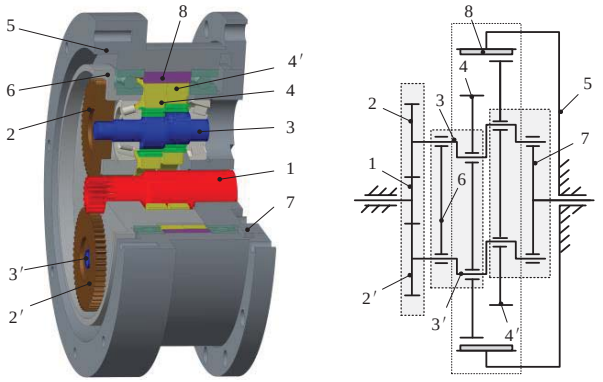

(a) RV reducer structure

(b) RV reducer transmission principle

1. Input shaft, 2. Planetary gear, 3. Crankshaft, 4. Cycloid gear, 5. Needle tooth shell, 6. Planet carrier, 7. Flange plate, and 8. Pin gear

Fig. 1. Schematic diagram of RV reducer structure.

2. RV Reducer Structure and Transmission Error

2.1. Transmission Principle and Structure

An RV reducer is a two-stage transmission mechanism composed of K-H and K-H-V planetary transmissions, including an input shaft, planetary gear, a crankshaft, cycloid gear, a needle tooth shell, a planet carrier, a flange plate, a pin gear, etc.; its composition is shown in **Fig. 1(a)**. According to different occasions, the RV-40E reducer has six different installation configurations. This study takes the flange as the frame as an example to illustrate its transmission principle. The transmission principle is shown in **Fig. 1(b)**.

When the input shaft 1 rotates clockwise, the two planetary gears 2 and 2′ that are evenly distributed at 180° are revolved around the input shaft and rotate counterclockwise. Crankshafts 3 and 3′ are fixed to the planetary gears and their state of motion is the same as that of the planetary gear. The crankshafts are coupled to two equal-sized cycloid gears 4 and 4′ by a slewing bearing and the two cycloid gears are 180° out of phase. The rotation of the crankshaft 3 drives the cycloid gear to revolve around the center line of the needle tooth shell 5 and mesh with pin gear 8. The pin gear is placed in the tooth gap of the needle tooth shell and the needle tooth shell is fixed; the cycloid gear is subjected to the reverse meshing force of the pin gear. The rotation is the same as that of the input shaft. The rotation of the cycloid gear transmits the planet carrier 6 and the flange plate 7 through the bearings on the two crankshafts and the flange plate and the planet carrier are bolted together to rotate at the same speed as the output mechanism. The RV reducer has become mainstream for industrial robots because of its compact structure, large reduction ratio, smooth motion, and high torsional stiffness and reliability.

2.2. Dynamic Transmission Error

The RV reducer transmission error can be divided into dynamic transmission and static transmission errors. The dynamic transmission error is mainly caused by the elastic deformation of the internal components of the reducer and the combination of machining error, clearance, and assembly error caused by the load. Static transmission error is the error that occurs when there is no load and mainly occurs due to factors related to the manufacturing and assembly accuracy of the reducer, such as machining error, clearance, and assembly error. The RV reducer transmission error can be reflected by the angle error. During the actual RV reducer working process, the dynamic influence of the elastic deformation of the part and the load on the transmission error of the RV reducer cannot be ignored. However, because of the unique structure of the RV reducer, factors affecting the dynamic transmission error are numerous and complicated. There is a coupling relationship, and theoretical analysis is quite difficult. For the RV reducer nonlinear factors, the elastic deformation of components, the load, and the stiffness of the cycloidal wheel, the finite element analysis method combined with various influencing factors is used to establish multiple virtual prototype models that can accurately predict the RV reducer dynamics. The angle error is the difference between the theoretical output angle and the actual output angle; the calculation formula is as follows:

$$\varphi_{\mathrm{er}} = \frac{\varphi_{\mathrm{in}}}{i} - \varphi_{\mathrm{out}}, \quad \ldots\ldots\ldots\ldots\ldots\ldots (1)$$

where φ_{er} is the angle error, φ_{in} is the input rotation angle of the input shaft, φ_{out} is the actual rotation angle of the output axis, and i is the reduction ratio.

3. Simulation of RV Reducer Dynamic Transmission Error

The Taguchi method is a test method that uses a normalized orthogonal table to achieve multi-factor and multi-level equilibrium matching, performs fewer representative tests, analyzes the sensitivity of each factor to the target, and finds a test technique with a good combination of factors. Many scholars use the Taguchi method to design experiments. Tanaka and Kitamura proposed an improvement of milling for thermo-plastic carbon fiber reinforced plastic (CFRP) with a radius end mill. Based on the consideration of the schematic model and experiments using the Taguchi method, the improved milling conditions were examined [19]. Wu et al. proposed a new method of using Ultrasonic Assisted fixed-abrasive Chemo-Mechanical Polishing (UA-CMP) to treat silicon wafer edges and the optimal processing conditions were experimentally determined using the Taguchi method [20]. The Taguchi method was used in this study to design the simulation test scheme for RV reducer dynamic transmission error.

3.1. Selection of Influential Factors

There are many influential factors affecting RV reducer transmission error, including elastic deformation of parts, load, manufacturing error, and clearance. As the transmission error of the involute planetary part has been reduced many times by the final output of the transmission ratio, the transmission error of the cycloid gear part is directly reflected in the whole machine error, which has a great influence on the total transmission error. Thus, the selection of influential factors for simulation is mainly driven by the secondary cycloidal transmission.

3.1.1. Selection of Elastic Deformation and Load Factors

The RV reducer is mostly used in the arm of industrial robots. Because of the need to overcome the gravity of the robot and the workpiece, the internal parts are prone to elastic deformation. The component elastic deformation is mainly related to the structure, material characteristics and load size of each component. The cycloid gear, pin gear, and crankshaft bearings are important components of the secondary drive of the RV reducer, as they carry the main load work process, and their elastic deformation directly reflects the transmission error. Therefore, the elastic deformation of the cycloidal, pin and arm bearings is selected as the influencing factor of the simulation. Because the bearing modeling is complicated, and the motion constraints are difficult, the bearings in the model are replaced by bushings. The actual working load of the RV reducer is always in a fluctuating state. The magnitude and volatility of the working load may have a certain influence on the RV reducer transmission error. Therefore, the working load part selects the two influencing factors of load size and fluctuation as simulation test factors.

3.1.2. Selection of Part Manufacturing Error

Because of the manufacturing error of the RV reducer parts, there are greater than ten manufacturing errors of the cycloidal wheel. It is difficult to study the manufacturing error of each part. Therefore, the influencing factors of the part manufacturing error are mainly selected based on the secondary cycloidal transmission according to the sensitivity of each part error to the transmission error. The existence of the manufacturing error of the parts causes a certain meshing clearance between the cycloid and pin gears, which is the main reason for the cycloidal transmission error. The manufacturing error of the main parts that causes the transmission error is as follows [21].

(1) Transmission error caused by the circle center radius error of pin gear $\Delta\varphi_1$:

$$\Delta\varphi_1 = \frac{2\delta r_p\sqrt{1-{K_1}^2}}{az_c}, \quad \ldots\ldots\ldots (2)$$

where δr_p is the circle center radius error of the pin gear [mm], a is the eccentricity of the crankshaft [mm], z_c is the number of cycloid gear teeth, and K_1 is the curtate ratio.

(2) Transmission error caused by the pin gear radius error $\Delta\varphi_2$:

$$\Delta\varphi_2 = -\frac{2\delta r_{r_p}}{az_c}, \quad \ldots\ldots\ldots\ldots (3)$$

where δr_{r_p} is the pin gear radius error [mm].

(3) Transmission error caused by the circular position error of the pin gear hole $\Delta\varphi_3$:

$$\Delta\varphi_3 = \frac{2K_1\delta t_\Sigma}{az_c}, \quad \ldots\ldots\ldots\ldots (4)$$

where δt_Σ is the circular position error of the pin gear hole [mm].

(4) Transmission error caused by the matching clearance between the pin gear and pin gear hole $\Delta\varphi_4$:

$$\Delta\varphi_4 = \frac{\delta j}{az_c}, \quad \ldots\ldots\ldots\ldots (5)$$

where δj is the matching clearance between the pin gear and pin gear hole.

(5) Transmission error caused by the modification of the cycloidal wheel $\Delta\varphi_5$:

$$\Delta\varphi_5 = \frac{2\Delta r_{r_p}}{az_c} - \frac{2\Delta r_p}{az_c}\sqrt{1-{K_1}^2}, \quad \ldots\ldots (6)$$

where Δr_{r_p} is the amount of equidistant modification of the cycloid gear [mm] and Δr_p is the amount of radial-moving modification of cycloid gear [mm].

(6) Transmission error caused by the radial ring runout of the cycloid gear $\Delta\varphi_6$:

$$\Delta\varphi_6 = \frac{\Delta F_{t1}}{2az_c}, \quad \ldots\ldots\ldots\ldots (7)$$

where ΔF_{t1} is the radial ring runout error of the cycloid gear [mm].

(7) Transmission error caused by the tooth pitch cumulative error of the cycloid gear $\Delta\varphi_7$:

$$\Delta\varphi_7 = -\frac{K_1\Delta F_P}{az_c}, \quad \ldots\ldots\ldots\ldots (8)$$

where ΔF_P is the tooth pitch cumulative error of the cycloid gear [mm].

(8) Transmission error caused by the cycloid gear modification error and the crankshaft eccentricity error $\Delta\varphi_8$:

The tooth profile modification amount of the cycloid gear has been provided at the time of design. However, because of the existence of machining errors, the modification error of the cycloidal wheel is inevitable. The profile modification error of the cycloid gear is based on the actual profile modification of the cycloid gear and theoretical repair, which is the deviation value between the actual modification amount and the theoretical modification amount of the cycloid gear. For Eq. (6), the Taylor series is expanded to (Δr_{r_p}, Δr_p, a), and the square of the error is omitted as follows:

$$\Delta\varphi_8 = \frac{2}{az_c}\delta\Delta r_{r_p} - \frac{2\delta\Delta r_p}{az_c}\sqrt{1-{K_1}^2} - \left[\frac{2\Delta r_{r_p}}{a^2z_c} - \left(\frac{2z_c}{a{r_p}^2\sqrt{1-{K_1}^2}} + \frac{2\sqrt{1-{K_1}^2}}{a^2z_c}\right)\Delta r_p\right]\delta a. \quad \ldots\ldots\ldots\ldots (9)$$

where δa is the eccentricity error [mm], $\delta\Delta r_p$ is the equidistant modification error [mm], and $\delta\Delta r_{r_p}$ is the radial-moving modification error [mm].

Let

$$k_n = \frac{\Delta r_{r_p}}{a^2z_c} - \left(\frac{z_c}{a{r_p}^2\sqrt{1-{K_1}^2}} + \frac{\sqrt{1-{K_1}^2}}{a^2z_c}\right)\Delta r_p,$$

then:

$$\Delta\varphi_8 = \frac{2}{az_c}\delta\Delta r_{\rho\pi} - \frac{2\delta\Delta r_p}{az_c}\sqrt{1-{K_1}^2} - 2k_n\delta a. \quad (10)$$

Calculating the mean value of the transmission error caused by the transmission part of the cycloidal wheel according to the mean value we obtain the following:

$$\Delta\overline{\varphi} = \frac{180\times 60}{\pi}\sum_{j=1}^{8}\Delta\varphi_j. \quad \ldots\ldots\ldots (11)$$

According to the influence model of the error factors on the transmission error in the aforementioned formula, according to the sensitivity analysis principle, it is for the following function:

$$Y = Y(x_1, x_2, \ldots, x_n), \quad \ldots\ldots\ldots\ldots (12)$$

when there is an error in x_i, Δx_i is expanded by Taylor series in a small case, and the error calculation equation is obtained by omitting the items above the linear:

$$Y(x_1+\Delta x_1, x_2+\Delta x_2, \ldots, x_n+\Delta x_n) = Y(x_1, x_2, \ldots, x_n) + \left(\frac{\partial Y}{\partial x_1}\Delta x_1 + \frac{\partial Y}{\partial x_2}\Delta x_2 + \cdots + \frac{\partial Y}{\partial x_n}\Delta x_n + \Delta x_n\right). \quad (13)$$

The error of the function $Y(x_1, x_2, \ldots, x_n)$ is as follows:

$$\Delta Y = \frac{\partial Y}{\partial x_1}\Delta x_1 + \frac{\partial Y}{\partial x_2}\Delta x_2 + \cdots + \frac{\partial Y}{\partial x_n}\Delta x_n. \quad \ldots (14)$$

The sensitivity index is defined as follows:

$$S_i = \frac{\partial Y/\partial x_i}{\partial Y/\partial x_0}, \quad \ldots\ldots\ldots\ldots (15)$$

where $\partial Y/\partial x_0$ is an input error parameter as a reference. Because it is a constant when the value is determined, Eq. (14) can be written as follows:

$$\Delta Y = g_1\Delta x_1 + g_2\Delta x_2 + \cdots + g_n\Delta x_n. \quad \ldots\ldots (16)$$

Similarly, the sensitivity index can be expressed as follows:

$$S_i = \frac{g_i}{g_0}. \quad \ldots\ldots\ldots\ldots (17)$$

It is known that the eccentricity a is 1.5 mm, the number of trochoidal teeth z_c is 39, and the curtate ratio of the cycloid gear K_1 is 0.73. Sensitivity analysis was performed for each influential factor, and the analysis results are shown in **Table 1**. From the table, we can see the equidistant modification of the cycloid gear, the radial runout of the cycloidal gear, the circumferential position error of the pin gear hole, the radial-moving modification of the cycloid gear, and the radius error of the center circle of the pin gear. All of them are sensitive to the influence of the transmission error. Because it is difficult to add the error parameters such as the radial ring runout of the cycloid gear and the cumulative error of the cycloid gear pitch during the three-dimensional (3D) modeling process, the selected simulation test factors should be compared to other influencing factors. Therefore, the part error part selects the pin gear radius error, the pin gear center circle radius error, the crank axis eccentricity error, the cycloid gear equidistant modification amount, and the cycloid gear radial-moving modification amount as the simulation test factors.

3.1.3. Selection of Part Matching Clearance

In the RV reducer, the main matching clearance of parts includes the solar wheel planetary gear meshing clearance, the bearing clearance between the crank bore of the cycloid gear and the crank shaft, the bearing clearance between the crankshaft hole of the planetary frame and the crank shaft, the bearing clearance between the planetary frame and the machine frame, the meshing clearance between the cycloidal gear and the pin gear, and the mating clearance between the pin gear and the nee-

Table 1. Error sensitivity analysis of parts.

Serial number	Error parameter	Error value [mm]	Coefficient		Sensitivity index
1	Circle center radius error of pin gear	0.025	$\sqrt{1-K_1{}^2}$	0.68	1
2	Pin gear radius error	0.015	-1	-1	-1.47
3	Circular position error of pin gear hole	0.01	K_1	0.73	1.07
4	Matching clearance between the pin gear and the pin gear hole	0.002	0.5	0.5	0.735
5	Amount of equidistant modification of cycloid gear	0.016	1	1	1.47
6	Amount of radial-moving modification of cycloid gear	0.026	$-\sqrt{1-K_1{}^2}$	0.68	-1
7	Radial ring runout of cycloid gear	0.014	0.25	0.25	0.368
8	Tooth pitch cumulative error of the cycloid gear	0.015	$-K_1/2$	-0.365	-0.535
9	Eccentricity error	0.005	K_n	0.00005	0.00007

dle tooth shell. Because the part matching clearance in the secondary transmission of the cycloidal wheel is directly transmitted to the output mechanism, the bearing in the virtual prototype model is replaced by a bushing, such that the matching clearance of parts only selects the clearance of the inner hole of the cycloid gear and the bushing of the rotating arm, the clearance between the crank shaft and the bushing of the rotating arm, the clearance between the crank shaft and the support bushing, the clearance between the upper support bushing and the planetary frame, and the clearance between the lower support bushing and the flange plate as the simulation test factors.

3.2. Simulation Scheme

The simulation scheme was developed based on the orthogonal test method. First, the factor level table is established according to the RV-40E type reducer drawing data and the actual manufacturing situation, as shown in **Table 2**. To prevent interference between parts, the radius error of the pin gear, the eccentricity error of the crank shaft, and the amount of equidistant modification of the cycloid gear are negative, and the circle center radius error of the pin gear and the distance of the cycloid gear are positive. Then, the simulation scheme is developed. Because 4 of the 15 influencing factors are two levels and 11 of them are three levels, a hybrid orthogonal table L36 ($2^4 \times 3^{11}$) is used to establish the simulation scheme, as shown in **Table 3**. Basic design dimensions of the virtual prototype of the RV 40-E reducer are shown in **Table 4**.

3.3. Establishment of a Virtual Prototype

(1) *Assembly modeling.* It is difficult to construct a complex 3D model in ADAMS; thus, a 3D model of the RV reducer is built using CREO according to the data of the simulation scheme. Taking the crankshaft of the first group of virtual prototypes as an example, the eccentricity error of the crankshaft is 0.02 mm and the original crankshaft eccentricity is 1.5 mm. To prevent interference between the model parts after adding the eccentricity error, the crankshaft model eccentricity modeling

Table 2. Factor level table.

Factor		Level [mm]		
		1	2	3
A	Whether the cycloid gear is a flexible body	Y	N	–
B	Whether the pin gear is a flexible body	Y	N	–
C	Whether the arm bushing is a flexible body	Y	N	–
D	Whether the load is volatility	Y	N	–
E	Load size [N·m]	200	300	400
F	Pin gear radius error	0.01	0.02	0.03
G	Crankshaft eccentricity error	0.005	0.01	0.015
H	Pin gear center circle radius error	0.01	0.02	0.03
I	Cycloid gear equidistant modification amount	0.016	0.032	0.048
J	Cycloid gear radial-moving modification amount	0.026	0.052	0.078
K	Crankshaft and arm bushing clearance	0	0.005	0.01
L	Support bushing and flange clearance	0	0.005	0.01
M	Cycloid inner hole and arm bushing clearance	0	0.005	0.01
N	Support bushing and carrier clearance	0	0.005	0.01
O	Crankshaft and support bushing clearance	0	0.005	0.01

size is 1.48 mm, and the 3D model of other parts is built similar to the crankshaft. Some components were simplified during the modeling process, including the bearing was replaced by a shaft bushing, neglecting the fine structure such as chamfer bolts, consolidation by the pin, key, and bolt connection. Sealing rings, gaskets, etc. were removed as they have no influence on the study. Eq. (18) of the cycloidal line was established in CREO and the cycloidal profile curve was obtained by mapping. One-half of the cycloid gear profile of the complete cycloid gear is drawn by the equation. Then, the 3D model of the cycloid gear can be obtained by mirroring, array, and stretching commands. The solid model of all parts was assembled to obtain the RV reducer assembly model.

Table 3. Simulation results.

Simulation number	Simulation scheme of virtual prototype															Simulation results
	A	B	C	D	E	F	G	H	I	J	K	L	M	N	O	Transmission error [′]
1	1	1	1	1	1	1	1	1	1	1	1	1	1	1	1	0.786
2	1	1	1	1	2	2	2	2	2	2	2	2	2	2	2	1.137
3	1	1	1	1	3	3	3	3	3	3	3	3	3	3	3	2.267
4	1	1	1	1	1	1	1	1	2	2	2	2	3	3	3	1.094
5	1	1	1	1	2	2	2	2	3	3	3	3	1	1	1	1.000
6	1	1	1	1	3	3	3	3	1	1	1	1	2	2	2	1.820
7	1	1	2	2	1	1	2	3	1	2	3	3	1	2	2	1.438
8	1	1	2	2	2	2	3	1	2	3	1	1	2	3	3	0.967
9	1	1	2	2	3	3	1	2	3	1	2	2	3	1	1	0.760
10	1	2	1	2	1	1	3	2	1	3	2	3	2	1	3	0.920
11	1	2	1	2	2	2	1	3	2	1	3	1	3	2	1	0.996
12	1	2	1	2	3	3	2	1	3	2	1	2	1	3	2	1.669
13	1	2	2	1	1	2	3	1	3	2	1	3	3	2	1	1.439
14	1	2	2	1	2	3	1	2	1	3	2	1	1	3	2	1.678
15	1	2	2	1	3	1	2	3	2	1	3	2	2	1	3	1.318
16	1	2	2	2	1	2	3	2	1	1	3	2	3	3	2	0.782
17	1	2	2	2	2	3	1	3	2	2	1	3	1	1	3	1.963
18	1	2	2	2	3	1	2	1	3	3	2	1	2	2	1	1.900
19	2	1	2	2	1	2	1	3	3	3	1	2	2	1	2	2.059
20	2	1	2	2	2	3	2	1	1	1	2	3	3	2	3	0.602
21	2	1	2	2	3	1	3	2	2	2	3	1	1	3	1	1.620
22	2	1	2	1	1	2	2	3	3	1	2	1	1	3	3	1.880
23	2	1	2	1	2	3	3	1	1	2	3	2	2	1	1	0.733
24	2	1	2	1	3	1	1	2	2	3	1	3	3	2	2	1.460
25	2	1	1	2	1	3	2	1	2	3	3	1	3	1	2	0.674
26	2	1	1	2	2	1	3	2	3	1	1	2	1	2	3	1.762
27	2	1	1	2	3	2	1	3	1	2	2	3	2	3	1	1.190
28	2	2	2	1	1	3	2	2	2	1	1	3	2	3	1	0.865
29	2	2	2	1	2	1	3	3	3	2	2	1	3	1	2	0.977
30	2	2	2	1	3	2	1	1	1	3	3	2	1	2	3	0.769
31	2	2	1	2	1	3	3	3	2	3	2	2	1	2	1	1.697
32	2	2	1	2	2	1	1	1	3	1	3	3	2	3	2	1.237
33	2	2	1	2	3	2	2	2	1	2	1	1	3	1	3	0.861
34	2	2	1	1	1	3	1	2	3	2	3	1	2	2	3	1.566
35	2	2	1	1	2	1	2	3	1	3	1	2	3	3	1	1.642
36	2	2	1	1	3	2	3	1	2	1	2	3	1	1	2	0.989
k1	1.330	1.292	1.295	1.301	1.267	1.346	1.297	1.072	1.102	1.150	1.441	1.310	1.437	1.087	1.219	$T =$ 52.979
k2	1.255	1.293	1.289	1.283	1.224	1.172	1.249	1.201	1.232	1.307	1.235	1.285	1.309	1.382	1.327	
k3	–	–	–	–	1.385	1.358	1.331	1.604	1.543	1.419	1.200	1.281	1.130	1.408	1.331	
Range R	0.075	0.001	0.005	0.018	0.161	0.185	0.082	0.532	0.441	0.270	0.241	0.030	0.308	0.321	0.112	
Factor order	H>I>N>M>J>K>F>E>O>G>A>L>D>C>B															
Optimal level	2	2	2	2	2	2	2	1	1	1	3	3	3	1	1	
Optimization	$A_2B_2C_2D_2E_2F_2G_2H_1I_1J_1K_3L_3M_3N_1O_1$															

Table 4. Basic design dimensions of the virtual prototype.

Speed ratio			121		
Stage I	Sun gear	Planet gear	Stage II	Cycloid gear	Pin gear
Module [mm]	1.25		Eccentricity [mm]	1.5	
Tooth number	18	54	Tooth number	39	40
Tooth width [mm]	7		Tooth width [mm]	15	32
Pressure angle [°]	20		Pin gear radius [mm]	–	3
Modification coefficient	0.469	−0.505	Pin gear center circle radius[mm]	–	82

Table 5. RV reducer part material properties.

Part Name	Material	Elastic modulus E [N·mm^{-2}]	Material density ρ [kg·mm^{-3}]	Poisson's ratio
Input shaft	15CrMo	2.12×10^{11}	7.88×10^{3}	0.284
Planetary gear	38CrMoAl	2.11×10^{11}	7.85×10^{3}	0.277
Planet carrier	ZG65Mn	1.98×10^{11}	7.85×10^{3}	0.230
Cycloid gear	20CrMnMo	2.07×10^{11}	7.87×10^{3}	0.254
Crankshaft	20CrMnMo	2.07×10^{11}	7.87×10^{3}	0.254
Needle tooth shell	GCr15	2.19×10^{11}	7.83×10^{3}	0.300
Pin gear	QT500-7	1.68×10^{11}	7.25×10^{3}	0.240
Flange	ZG65Mn	1.98×10^{11}	7.85×10^{3}	0.230

$$\begin{cases} x = (r_p+\Delta r_p)\left(\sin(360\cdot t)-\dfrac{k}{z_b}\sin(z_c\cdot 360\cdot t)\right) \\ \quad +\dfrac{(r_p+\Delta r_{r_p})\,(k\sin(z_c\cdot 360\cdot t)-\sin(360\cdot t))}{\sqrt{1+k^2-2k\cos(z_c\cdot 360\cdot t)}} \\ y = (r_p+\Delta r_{r_p})\left(\cos(360\cdot t)-\dfrac{k}{z_b}\cos(z_c\cdot 360\cdot t)\right) \\ \quad +\dfrac{(r_p+\Delta r_{r_p})\,(-k\cos(z_c\cdot 360\cdot t)-\cos(360\cdot t))}{\sqrt{1+k^2-2k\cos(z_c\cdot 360\cdot t)}} \\ k = \dfrac{a\times z_c}{r_p+\Delta r_p} \end{cases} \quad (18)$$

where t is the system variable in the CREO relation ($0 \le t \le 1$), r_p is the center circle radius of the pin gear, z_b is the number of the pin gear, r_{r_p} is the radius of the pin gear, z_c is the number of the cycloid gear, a is the eccentricity, Δr_p is the amount of equidistant modification, and Δr_{r_p} is the amount of radial-moving modification.

(2) *Defining model material characteristics.* The intermediate format model file is imported into the ADAMS software through the File/Import command, and the component materials are defined. The elastic modulus, density, Poisson's ratio, and other material characteristics of each part based on the ADAMS contact collision theory are shown in **Table 5**.

Fig. 2. Cycloid wheel finite element mesh mode.

Table 6. Virtual prototype constraint and contact relation.

Constraints and numbers	Part 1	Part 2
Fixed pair (2)	Pin gear, Needle tooth shell	Ground
Fixed pair (1)	Planet carrier	Flange plate
Fixed pair (2)	Planetary gear	Crankshaft
Rotating pair (2)	Input shaft, Planet carrier	Ground
Rotating pair (2)	Planetary gear	Ground
Gear pair (2)	Planetary gear rotary pair	Input shaft rotary pair
Plane pair (4)	Cycloid gear	Rotary arm bushing
Contact (80)	Pin gear	Cycloid gear
Contact (8)	Crankshaft, Cycloid	Rotary arm bushing
Contact (2)	Input shaft	Planet carrier
Contact (2)	Bearing bushing	Planet carrier
Contact (2)	Bearing bushing	Flange plate

(3) *Replacing flexible body parts.* The 3D model of the cycloid gear, pin gear, and crank shaft bushings is imported into ANSYS for modal calculation to generate modal neutral component files. The finite element model of the cycloidal wheel is shown in **Fig. 2**. The flexible body is replaced in ADAMS according to the simulation scheme to establish a rigid-flexible coupled virtual prototype model.

(4) *Analyzing constraint relationships.* To ensure the correct motion of each component, the construction of the virtual prototype needs to provide constraints or contact relationships according to the component motion trajectories. Through the motion and contact analysis of the RV reducer components, the constraint and contact relationship of each component are determined as shown in **Table 6**.

Component material properties and constraint relationships area are added to obtain a virtual prototype as shown in **Fig. 3** that contains 58 parts, 15 constraints, and 94 contacts and the rotational drive input speed function is set as follows:

$$F(time) = 7000d \times time \times \text{step}(time,\ 0,\ 1,\ 0,\ 1). \quad (19)$$

According to the simulation test scheme, the load torque is set and the fluctuation amplitude is 10% of the rated

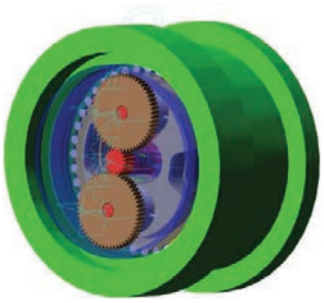

Fig. 3. Virtual prototype.

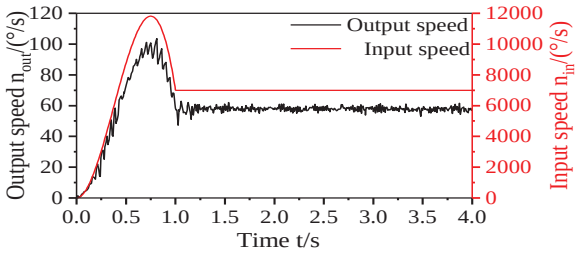

Fig. 4. Input and output speed curve of virtual prototype.

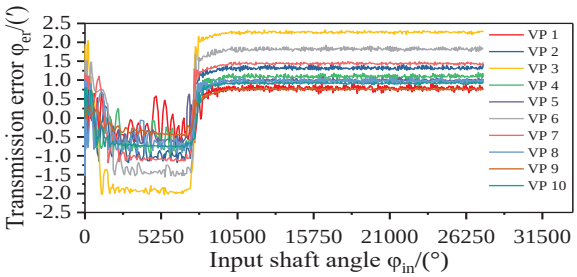

Fig. 5. Virtual prototype transmission error curves.

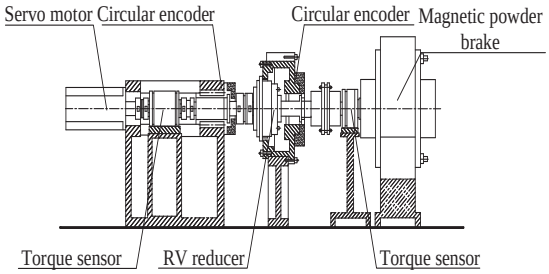

Fig. 6. Diagram of RV transmission error test platform.

load to define the load torque function with and without fluctuation as follows:

$$F(time) = \text{step}(time,\ 1,\ 1.5,\ 0,\ X) + 41.2\sin(40\pi time), \quad . \ . \ . \ . \quad (20)$$

$$F(time) = \text{step}(time,\ 1,\ 1.5,\ 0,\ X), \quad . \ . \ . \quad (21)$$

where X is the load size and *time* is that spent for the simulation.

The 4-s simulation time is defined, and the number of steps is simulated in 100 steps. The input shaft input speed and the planet carrier output speed curve are measured as shown in **Fig. 4**. After 1.5 s, the model motion is stable, the input shaft speed is 7000°/s, and the planetary carrier speed is 57.745°/s. Their ratio is 121.224, which is consistent with the theoretical transmission ratio 121, proving that the model is accurate and reliable.

3.4. Simulation Analysis

The transmission error can be calculated using Eq. (1). In ADAMS, the input carrier and planet carrier rotation angle are measured and then a function established as follows:

$$\text{FUNCTION} = \frac{JOINT\_1\_MEA\_1}{121} - JOINT\_2\_MEA\_1, \quad . \quad (22)$$

where FUNCTION is the angle error, *JOINT_1_MEA_1* is the rotation angle of the input shaft, and *JOINT_2_MEA_1* is the rotation angle of the output planet carrier.

According to the simulation scheme, the virtual prototype model is established and imported into ADAMS to measure the transmission error of each group. The curves of the input shaft rotation angle and transmission error of the top 10 sets of simulation results are shown in **Fig. 5**. Because there are too many virtual prototype simulation groups, other virtual prototype transmission error curves are not listed. The virtual prototype is loaded within 0–1.5 s of the simulation run and the model movement is unstable. The mean value of the virtual prototype transmission error curve after steady motion is chosen as the evaluation index of the transmission error, and the simulation test results are shown in **Table 3**.

3.5. Experimental Verification of the Simulation Method

To verify the reliability of the virtual prototype research method, the actual prototype assembly and transmission error measurement are conducted according to the virtual prototype experimental data. The RV transmission error tester is mainly composed of a servo motor, torque sensor, reducer seat, input shaft, output shaft, circular grating encoder, and magnetic powder brake; the functional diagram is shown in **Fig. 6**. The circular grating encoder is used to collect the RV reducer input and output rotation angles. The torque sensor can measure the input and output torque and monitor the load applied by the magnetic powder brake.

To qualitatively study the influential trend of the part matching clearance, the bearing in the virtual prototype is replaced by a bushing, and the case in which the matching clearance is zero is considered. However, because of the existence of a bearing clearance, there is always a certain clearance between the bearing and shaft. Therefore, the second, third, and fourth groups of the virtual prototyping machines with clearance between the bushing and the shaft are selected to measure the actual trans-

Table 7. Test prototype part information sheet.

Part size [mm]	TP 1	TP 2	TP 3
Pin gear radius	2.980	2.970	2.990
Eccentricity	1.490	1.485	1.495
Pin gear center circle radius	82.020	82.030	82.010
Cycloidal gear equidistant modification amount	0.032	0.048	0.032
Cycloid gear radial moving modification amount	0.052	0.078	0.052
Bearing clearance	0.005	0.010	0.005/0.010

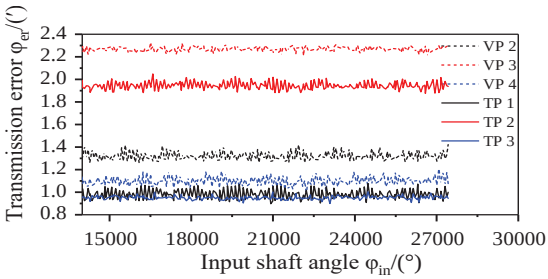

Fig. 7. Comparison curve of transmission error between the test and virtual prototypes.

mission error. The first, second, and third test prototypes are assembled according to the part data in the orthogonal simulation scheme; the test prototype part information is shown in **Table 7**. The first, second, and third test prototypes correspond to the second, third, and fourth groups of virtual prototypes in the orthogonal simulation scheme. Specifically, bearings with a clearance of 0.005 mm were selected in test prototype 1, bearings with a clearance of 0.01 mm in test prototype 2, and bearings with a clearance of 0.005 mm in support bearing clearance and rotary arm bearing clearance of 0.01 mm in test prototype 3. The RV reducer input shaft connects with the servo motor and circular encoder through the coupling, and the output shaft connects the circular grating encoder and magnetic powder brake. The servo motor speed is adjusted to 1200 r/min and the load is applied to the output shaft through the magnetic powder brake. When the RV reducer is in stable operation, measurement of experimental data begins.

The transmission error measurement curve is compared to the virtual prototype simulation curve as shown in **Fig. 7**. The RV reducer transmission error test prototype is 0.978′, 1.942′, and 0.949′, respectively. The error between the simulation result and the actual measurement is 13.98%, 14.38%, and 13.21%, respectively. The source of the simulation error is mainly due to the friction not considered in the virtual prototype and the bearing is replaced by the bushing; however, the simulation error is still within an acceptable range. This indicates that the virtual prototype simulation method is feasible and the simulation results have high reliability.

4. Analysis of Simulation Results

4.1. Range Analysis

Range analysis uses the data difference to analyze the problem. By comparing the average range of the experimental results, the main factors affecting the test indicators are determined. The principle is that when considering the effect of single factor A on the results, it is considered that the influence of other factors on the results is balanced, and the difference in the factor A levels is caused by factor A itself. The greater the difference, the greater the influence of this factor on the experimental indicators. The range R of each factor is calculated using Eq. (23) as follows:

$$\begin{cases} R = \max\{k_i\} - \min\{k_i\} \\ k_i = \dfrac{K_i}{n} \\ T = \sum k_i \end{cases} \quad \ldots\ldots\ldots \quad (23)$$

where R is the range, i is the number of factors, k_i is the mean of the sum of the transmission errors corresponding to the i level, K_i is the sum of the transmission errors corresponding to the i level, n is the level of any column in the number of occurrences, and T is the sum of the transmission errors.

The result of the range analysis of the test results is shown in **Table 3**. The center circle radius error of the pin gear has the greatest influence on the RV reducer dynamic transmission error. The range of the equidistant modification amount of the cycloid gear is 0.441, indicating that the cycloidal gear equidistant modification amount is the second major influence factor of transmission error. The range of the clearance between the upper support bushing and the carrier gap is 0.321, which is the third in the factor sequence. The range of the elastic deformation of the pin gear is 0.001, indicating that the elastic deformation of the pin gear has the least influence on the RV reducer dynamic transmission error. According to the range magnitude of each influential factor, the sensitivity sequence of each factor of the RV reducer dynamic transmission error is as follows: H>I>N>M>J>K>F>E>O>G>A>L>D>C>B. The optimal combination is as follows: $A_2B_2C_2D_2E_2F_2G_2H_1I_1J_1K_3L_3M_3N_1O_1$.

4.2. Influential Factor Analysis

4.2.1. Elastic Deformation and Part Load

To analyze the relationship among the elastic deformation of the part, the load, and the dynamic transmission error, the influence of the elastic deformation of the part and the load on the RV reducer dynamic transmission error is shown in **Fig. 8**.

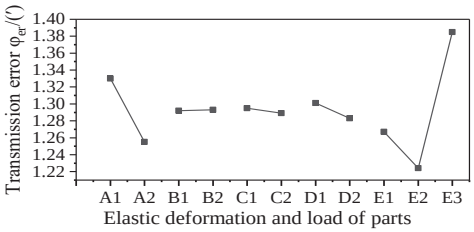

Fig. 8. Influence trend of elastic deformation and load transmission error.

Fig. 9. Influence trend of part manufacturing error and transmission error.

When the parts do not produce elastic deformation and the load does not fluctuate, the transmission error decreases. The cycloid gear elastic deformation has a significant influence on the transmission error, and the pin gear elastic deformation has the least influence on the transmission error. When the load increases from 200 N·m to 300 N·m, the transmission error decreases from 1.267′ to 1.224′. However, when the load continues to increase to 400 N·m, the transmission error increases to 1.385′, mainly because the change in the load causes the part to be elastically deformed, and the matching clearance between the parts changes accordingly. This result means that the influence of the load within the rated load on the RV reducer dynamic transmission error is nonlinear and the minimum transmission error is obtained only when a certain value is taken.

4.2.2. Part Manufacturing Error

The influence of part manufacturing error on the dynamic transmission error is shown in **Fig. 9**.

The influence of each component error on the RV reducer dynamic transmission error is obvious; the center circle radius error of the pin gear, the amount of equidistant modification of the cycloid gear, and the amount of radial-moving modification of the cycloid gear are positively correlated with the RV reducer transmission error. When the pin gear circle center radius error increases from 0.03 to 0.06 mm, the transmission error increases from 1.072′ to 1.201′. When the pin gear circle center radius error continues to increase to 0.09 mm, the transmission error increases to 1.604′. The amount of equidistant modification of the cycloid gear increases from 0.016 to 0.032 mm, and the transmission error increases from 1.102′ to 1.232′. When the amount of equidistant modification of the cycloid gear continues to

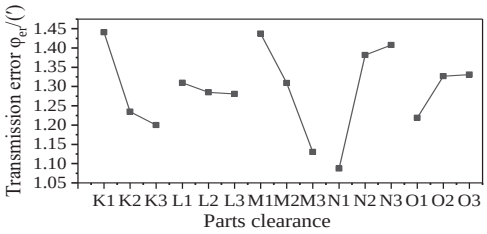

Fig. 10. Influence trend diagram of part clearance and transmission error.

increase to 0.048 mm, the transmission error increases to 1.543′. The pin gear radius error and crankshaft eccentricity error are nonlinearly related with the dynamic drive transmission error. When the pin gear radius error increases from 0.01 to 0.02 mm, the transmission error decreases from 1.346′ to 1.172′, the pin gear radius error increases to 0.03 mm, and the transmission error increases to 1.358′. The eccentricity error of the crankshaft increases from 0.010 to 0.02 mm, the transmission error decreases from 1.29′ to 1.243′. When the eccentricity error of the crankshaft continues to increase to 0.01 mm, the transmission error increases to 1.331′.

4.2.3. Part Clearance

The influence of the clearance of each part on the RV reducer dynamic transmission error is shown in **Fig. 10**.

The experimental results show that the relationship between the part clearance and the RV reducer dynamic transmission error is complicated; the clearance between the crankshaft and the arm bushing, the clearance between the lower support bushing and the flange, and the clearance between the inner diameter of the cycloid gear and the bushing are negatively correlated with the transmission error. However, the clearance between the lower support bushing and the flange has less influence on the transmission error. When the clearance between the crankshaft and the arm bushing increases from 0 to 0.005 mm, the transmission error decreases from 1.44′ to 1.235′. When the clearance continues to increase to 0.01 mm, the transmission error decreases to 1.2′. As the clearance between the upper support bushing and the carrier increases, the clearance between the crankshaft and the support bushing increases, the transmission error also gradually increases, but the first phase of the two clearances is larger than the second phase. When the clearance between the upper support bushing and the carrier is increased from 0 to 0.005 mm, the transmission error increases from 1.087′ to 1.382′; the increment is 0.295′. When the clearance continues to increase to 0.01 mm, the transmission error increases to 1.408′; the increment is 0.026′. When the clearance between the crankshaft and support bushing is increased from 0 to 0.005 mm, the transmission error increases from 1.219′ to 1.327′; the increment is 0.108′. When the clearance continues to increase to 0.01 mm, the transmission error increases to 1.331′; the increment is 0.004′.

Table 8. Variance analysis table.

Source of error	Degree of freedom	Adj SS	Adj MS	Value of F	Value of P
A	1	0.05048	0.050483	0.32	0.588
B	1	0.00001	0.000009	0.00	0.994
C	1	0.00026	0.000262	0.00	0.969
D	1	0.00287	0.002871	0.02	0.896
E	2	0.16684	0.083418	0.52	0.611
F	2	0.25863	0.129317	0.81	0.475
G	2	0.04092	0.020461	0.13	0.882
H	2	1.84987	0.924935	5.78	0.024
I	2	1.23223	0.616117	3.85	0.062
J	2	0.44015	0.220075	1.38	0.301
K	2	0.40770	0.203852	1.27	0.326
L	2	0.00613	0.003063	0.02	0.981
M	2	0.57386	0.286930	1.79	0.221
N	2	0.76371	0.381856	2.39	0.147
O	2	0.09656	0.048278	0.30	0.747
Error	9	1.43965	0.159961		
Total	35	7.32988			

4.3. Analysis of Variance

To more accurately evaluate the influence of various factors on the RV reducer dynamic transmission error, the variance analysis method is used to further estimate the error size and the importance of each factor on the test results is accurately estimated, thereby compensating for the range analysis shortcomings. The variance analysis of the simulation result was performed using Minitab; the analysis results are shown in **Table 8**.

In **Table 8**, Adj SS is the adjusted squared sum, Adj MS is the adjusted mean square and the value is equal to the corresponding Adj SS divided by the degree of freedom, and F is the statistic used for the hypothesis test. According to the statistics of the F value in the table A sequence, the degree of influence of various factors on the RV reducer dynamic transmission error can be obtained. The significance of the influencing factors can be checked by querying the F distribution table:

$$F_{0.1}(2,9) = 3.01. \quad \ldots \quad (24)$$

For a given level of significance $\alpha = 0.1$,

$$\begin{cases} F_{0.1}(2,9) < F_H \\ F_{0.1}(2,9) < F_I \end{cases} \quad \ldots \quad (25)$$

The error of the center circle radius of the pin gear and the amount of equidistant modification of the cycloid gear have a significant influence on the RV reducer dynamic transmission error. The influence of other factors is not significant. The elastic deformation of the pin gear has the least influence on the RV reducer dynamic transmission error. The results of the variance analysis and range analyses were the same and the correctness of the results of the range analysis was verified.

5. Conclusion

Through dynamic factor analysis and a simulation scheme design for a given RV reducer, CREO and ANSYS tools were used to construct a virtual prototype and imported into the ADAMS system for a multi-body dynamic rigid-flexible coupling simulation. A total of 36 sets of simulation test data was obtained. The analysis draws the following conclusions:

(1) Among the influencing factors of the RV reducer dynamic transmission error, the radius error of the center circle of the pin gear is the primary factor affecting the error followed by the equidistance of the cycloid gear. The elastic deformation of the pin gear has the least influence on the dynamic transmission error and it is necessary to control the center circle radius error of the pin gear.

(2) The elastic deformation of the part will increase the RV reducer dynamic transmission error. The elastic deformation of the cycloid gear has the greatest influence. When other mechanical properties are satisfied, the material with a higher rigidity is selected to reduce the impact of the elastic deformation of the cycloid gear on the RV reducer transmission accuracy.

(3) The influence of the part clearance on the RV reducer dynamic transmission error is complicated. The clearance between the crankshaft and the arm bushing, the lower support bushing and the flange clearance, and the inner diameter of the cycloid gear and the arm bushing clearance are negatively correlated with the RV reducer dynamic transmission error. The clearance between the upper support bushing and the clearance between the crankshaft and the support bushing are positively correlated with the RV reducer dynamic transmission error. Therefore, the arm bearings should be selected with appropriate clearance and the support bearing clearance should be as small as possible.

(4) The load size is nonlinearly related to the RV reducer dynamic transmission error. The change in the load causes elastic deformation of the part and the change in the matching clearance. There is a certain interaction among them. In addition, the load fluctuation will increase the RV reducer transmission error to a certain extent.

The RV reducer dynamic transmission error is also affected by factors such as rolling bearing precision and friction. However, the influence of rolling bearing and friction force is not considered in the virtual prototype model. Therefore, the interaction between factors and the selection of the optimal part clearance are yet to be determined.

Acknowledgements

This work was supported by the Natural Science Foundation Project of Zhejiang Province (Grant No. LY16G010013), National Natural Science Foundation of China (Grant No. 51605442), and National High-tech R&D Program of China (Grant No. 2015AA043002).

References:

[1] J. G. Blanche and D. C. H. Yang, "Cycloid Drives with Machining Tolerances," J. of Mechanisms Transmissions and Automation in Design, Vol.111, No.3, pp. 337-344, 1989.
[2] D. C. H. Yang and J. G. Blanche, "Design and application guidelines for cycloid drives with machining tolerances," Mechanism and Machine Theory, Vol.25, No.5, pp. 487-501, 1990.
[3] T. Hidaka, H. Y. Wang, T. Ishida, K. Matsumoto, and M. Hashimoto, "Rotational transmission error of K-H-V planetary gears with cycloid gear: first report, analytical method of the rotational transmission error," Trans. of the Japan Society of Mechanical Engineers C, Vol.60, No.570, pp. 645-653, 1994.
[4] T. Ishida, H. Y. Wang, T. Hidaka, and M. Hashimoto, "Rotational transmission error of k-h-v-type planetary gears with cycloid gears: second report, effects of manufacturing and assembly errors on rotational transmission error," Trans. of the Japan Society of Mechanical Engineers C, Vol.60, No.578, pp. 3510-3517, 1994.
[5] L. S. Han, Y. W. Shen, and H. J. Dong, "Research on Dynamic Transmission Error for 2K-V-type Drive based on Non-linear Dynamics," China Mechanical Engineering, Vol.18, No.9, pp. 1039-1042, 2007.
[6] W. D. He and L. J. Shan, "Research and Analysis on Transmission Error of RV Reducer Used in Robot," Recent Advances in Mechanism Design for Robotics, pp. 231-238, 2015.
[7] Z. J. Meng, L. Z. Jiang, and X. J. He, "Transmission Error Analysis of RV Reducer," J. of Residuals Science & Technology, Vol.13, No.8, pp. 333.1-333.6, 2016.
[8] L. J. Shan, Y. T. Liu, and W. D. He, "Analysis of Nonlinear Dynamic Accuracy on RV Transmission System," Advanced Materials Research, Vol.510, pp. 529-535, 2012.
[9] Y. G. Sun, X. F. Zhao, and F. Jiang, "Backlash analysis of RV Reducer based on Error Factor Sensitivity and Monte-Carlo Simulation," Int. J. of Hybrid Information Technology, Vol.7, No.2, pp. 283-292, 2014.
[10] H. M. Zhao, M. Wang, and L. L. Zhang, "Static Backlash Analysis and Study on Error Distribution of RV Reducer," J. of Tianjin University (Science and Technology), Vol.49, No.2, pp. 164-170, 2016.
[11] L. S. Han and F. Guo, "Global Sensitivity Analysis of Transmission Accuracy for RV-type Cycloid-pin Drive," J. of Mechanical Science and Technology, Vol.30, No.3, pp. 1225-1231, 2016.
[12] C. N. Li, J. Y. Liu, and T. Sun, "Study on Transmission Precision of Cycloid Pin Gear in 2K-V Planetary Drives," J. of Mechanical Engineering, Vol.37, No.4, pp. 61-65, 2001.
[13] X. Y. Chu, H. H. Xu, and X. M. Wu, "The method of selective assembly for the RV reducer based on genetic algorithm," ARCHIVE Proc. of the Institution of Mechanical Engineers Part C, J. of Mechanical Engineering Science, Vol.232, pp. 921-929, 2018.
[14] Y. H. Li, Q. Zang, and W. Li, "Robust Design of Decreasing RV Reducer's Transmission Error," Science Research Management, Vol.28, No.3, pp. 142-147, 2013.
[15] X. H. Wu and W. D. He, "Transmission Accuracy test and Virtual Prototype Simulation of the RV Reducer used in the Robot," J. of Machine Design, Vol.7, pp. 73-77, 2017.
[16] H. M. Liu, X. P. Qin, and J. J. Huang, "Simulation of Virtual Prototype and Research of Transmission Accuracy for RV Reducer," J. of Mechanical Transmission, Vol.40, No.5, pp. 55-60, 2016.
[17] B. Zhu, "Simulation and Analysis for Dynamical Transmission Precision of 2K-V Cycloid Pin Gear Reducer based on Multi-body System Dynamics," Chongqing University, 2015.
[18] H. Li, H. H. Xu, and K. Wu, "Analysis of Transmission Error of RV Reducer based on Orthogonal Experiment," J. of Mechanical Transmission, Vol.41, No.2, pp. 71-76, 2017.
[19] H. Tanaka and M. Kitamura, "Machinability of Thermo-Plastic Carbon Fiber Reinforced Plastic in Inclined Planetary Motion Milling," Int. J. Automation Technol., Vol.12, No.5, pp. 750-759, 2018.
[20] Y. Wu, W. Yang, M. Fujimoto, and L. Zhou, "Mirror Surface Finishing of Silicon Wafer Edge Using Ultrasonic Assisted Fixed-Abrasive CMP (UF-CMP)," Int. J. Automation Technol., Vol.7, No.6, pp. 663-670, 2013.
[21] Z. Zhang, G. R. Zhang, and H. W. Zhang, "The Calculation of Practical Handbook of Gear Design," Machinery Industry Press, pp. 941-945, 2010.

Name:
Shou-Song Jin

Affiliation:
Associate Professor, Zhejiang University of Technology

Address:
No.288 Liuhe Road, Xihu District, Hangzhou, Zhejiang 310023, China

Brief Biographical History:
1989 Received Master's degree (Mechanical Engineering) from Zhejiang University
1994 Received Ph.D. from Zhejiang University
1999- Associate Professor, Zhejiang University of Technology

Name:
Xiao-Tao Tong

Affiliation:
Master Candidate, College of Mechanical Engineering, Zhejiang University of Technology

Address:
No.288 Liuhe Road, Xihu District, Hangzhou, Zhejiang 310023, China

Brief Biographical History:
2016- Master Candidate, College of Mechanical Engineering, Zhejiang University of Technology

Name:
Ya-Liang Wang

Affiliation:
Senior Experimentalist, Zhejiang University of Technology

Address:
No.288 Liuhe Road, Xihu District, Hangzhou, Zhejiang 310023, China

Brief Biographical History:
2004 Received Master's degree (Mechanical Engineering) from Zhejiang University of Technology
2019 Received Ph.D. from Zhejiang University of Technology
2011- Senior Experimentalist, Zhejiang University of Technology

Main Works:
• "Design and application of cellular differential algorithm based on complete feedback from external population," Computer Integrated Manufacturing Systems, Vol.23, pp. 1679-1691, 2016.
• "Multi-objective optimization design of cycloid pin gear planetary reducer," Advances in Mechanical Engineering, Vol.9, pp. 1-10, 2017.